

油壓致動懸吊系統之滑動模式控制

Sliding-Mode Control for Hydraulic Actuating Suspension System

陳宏毅

Hung-Yi Chen

摘要

本論文針對油壓致動之懸吊系統，設計滑動模式控制器以進行控制。因為油壓致動懸吊系統具有非線性時變之特性，若要建立系統正確之動態數學模式是不容易的。因此，本研究利用透過系統鑑定所估測之線性數學模式來近似油壓致動懸吊系統，進一步設計滑動模式控制器來進行控制。透過實驗結果之驗證，本研究所設計之控制器能夠有效抑制車體在行經巔坡路面時所造成之車體振動量與加速度。

關鍵詞：滑動模式控制，油壓致動懸吊系統，系統鑑定。

ABSTRACT

This paper presents a practical design and implementation method of a sliding-mode controller (SMC) for a hydraulic actuating suspension system. Since the hydraulic actuating suspension system has nonlinear, time-varying behavior and complicated mathematical model, it is difficult to establish an accurate dynamic model for model-based control design. Hence, a linear time-varying model estimated from the system identification method is selected to approximate this nonlinear suspension system. The sliding-mode controller was designed based on the identified model for the hydraulic actuating suspension system. The experimental results show that the designed controller effectively suppresses the oscillation amplitude and acceleration of the vehicle sprung mass correlating to the road variation and external uncertainties.

Keywords: Sliding-mode control, Hydraulic actuating suspension system, System identification.

1. Introduction

Generally, a good suspension system should have the capability to reduce the car body displacement and acceleration, and maintain the right contact between tire and terrain. Since the vibration isolation capabilities of the traditional passive or semi-active suspension system are restricted, design a better quality active suspension system for achieving good ride comfort and maneuverability under various riding conditions is an important modern vehicle development objective. An active suspension system with additional actuating force and limited suspension travel can suppress the vehicle body oscillations due to road surface variation by using appropriate controller.

Since the active suspension system has

complicated and time-varying dynamics, the adaptive modern control theory was proposed to manipulate the control task and take care of the model dynamics variation. Alleyne and Hedrick [1] designed an adaptive controller with a modified adapting scheme to reduce the model error and cope with the system uncertainties. Rajamani and Hedrick [2] developed an adaptive observer for the parameter identification of the active suspension system. Kim [3] employed an indirect adaptive controller in a vehicle active suspension with a nonlinear hydraulic actuator. Chantranuwathana and Peng [4] proposed an adaptive robust force controller to tackle the actuator uncertainties of active suspension systems. Nguyen et al. [5] used H_∞ controller to take care of the road disturbance and adaptive backstepping control method to deal with the actuator nonlinearities. Smith and Wang [6] derived a

parameterized stable controller for a vehicle active suspension system with fixed prespecified closed-loop transfer function. Fialho and Balas [7] combined the linear parameter-varying control and nonlinear backstepping technique to design a road adaptive active suspension.

It is well known that the sliding-mode control can be used to handle the system nonlinear behavior, model uncertainties and external disturbance. The sliding-mode control algorithm was adopted to solve the problems of the hydraulic system nonlinearity and the road surface random variation of active suspension systems [8-10]. The sliding-mode control theory can employ a discontinuous control effort to drive the system toward a sliding surface, and then switching on that surface. Theoretically, it will gradually approach the control target, the origin of the phase plane.

Since it is difficult to establish an accurate dynamic model of a physically active suspension system for designing a model-based controller, and some of the hydraulic or pneumatic suspension systems are even difficult to establish the right model type for adaptive control design, this paper proposes a linear time-varying model estimated from the system identification method to approximate the nonlinear suspension system. Then, the model-based sliding-mode controller was designed based on the identified model for the hydraulic actuating suspension system.

This paper is organized as follows: Section 2 describes the dynamic model of the active suspension system. The approximate linear model and system identification process are presented in Section 3. The methodology of controller design is derived in Section 4. Section 5 describes the experimental results of the proposed controller. Final conclusions are presented in Section 6.

2. Active Suspension System Model

A quarter-car hydraulic actuating active suspension system shown in Figure 1 is built for

investigating the dynamic and control behavior. This suspension system includes mass-spring-damper mechanism and a hydraulic control loop. The hydraulic flow rate is regulated by a proportional flow valve. The dynamic behavior of this quarter-car suspension system can be simplified into a 2-DOF dynamic model as shown in Figure 2. The car body is considered as a sprung mass m_s . The damper b_s and the spring k_s constitute the passive component of this suspension system. The function of the tire is simulated by a spring with coefficient k_t and unsprung mass m_u . The actuating force F_a is generated by the hydraulic actuator and its magnitude is bounded by some known value. The variables Z_s and Z_u represent the vertical displacements of sprung mass and unsprung mass, respectively. Z_r is the vertical profile of road surface.

If the tire is always contacted with the road surface and the suspension travel is below its physical limit, the dynamic equations of this quarter-car active suspension system can be described as

$$m_s \ddot{Z}_s + b_s (\dot{Z}_s - \dot{Z}_u) + k_s (Z_s - Z_u) = F_a - F_f \quad (1)$$

$$m_u \ddot{Z}_u + b_s (\dot{Z}_u - \dot{Z}_s) + k_s (Z_u - Z_s) + k_t (Z_u - Z_r) = -F_a + F_f \quad (2)$$

where F_a and F_f are the hydraulic actuating force and the hydraulic friction force, respectively. These two forces can be derived from the dynamics of electro-hydraulic servo system. The hydraulic actuating force, F_a , is a nonlinear function of the control input voltage, suspension travel, cylinder pressure, etc. Its time derivative can be represented as [11]

$$\begin{aligned} \dot{F}_a(t) &= \dot{P}_L(t) A_p \\ &= A_p (4B/V_t) [K_s(t) K_u(t) - C_T P_L(t) - A_p (\dot{Z}_s(t) - \dot{Z}_u(t))] \end{aligned} \quad (3)$$

where A_p is the cross section area of hydraulic cylinder, $P_L(t)$ is the cylinder differential pressure, K_v is the servovalve gain, K_s is the servovalve flow gain, V_t is the total compressed volume, B is the bulk modulus of the hydraulic oil, C_T is the total leakage coefficient and $u(t)$ is the servovalve control voltage. The hydraulic friction force, F_f , is a nonlinear function of the external load, stick-slip friction and Coulomb friction. It is complicated and difficult to model and estimate. To simplify this model description, the system dynamics can be represented as the following third order model.

$$\ddot{x}_1(t) = f(X, t) + g(t)u(t) + d(t) \quad (4)$$

where $x_1 = Z_s$ is the sprung mass displacement, X is the state vector, $f(X, t)$ is a function of state variables, $g(t)$ is the control gain, $d(t)$ is the system uncertainty and disturbance, and $u(t)$ is the servovalve control voltage.

3. System Identification

In order to design the model-based sliding-mode controller for the quarter-car active suspension system, a dynamic model is estimated based on input-output data of the system. A pseudo-random-binary-sequences (PRBS) signal with appropriate amplitude is chosen as the input signal to excite the suspension system. The transfer function $M(q)$ that describes the relationship between voltage input and sprung mass position output can be represented as an auto-regressive (ARX) model.

$$M(q) = \frac{B(q)}{A(q)} \quad (5)$$

where $A(q) = 1 + a_1q^{-1} + \dots + a_{n_a}q^{-n_a}$, $B(q) = b_1q^{-1} + \dots + b_{n_b}q^{-n_b}$ and q is the shift operator. Based on previous system dynamics

derivation, equation (4), a third order transfer function model is selected and identified by using the MATLAB's identification toolbox [12].

$$M(q) = \frac{12820}{q^3 + 60.14q^2 + 1487q + 2824} \quad (6)$$

The model estimation output and the system experimental output under the PRBS input voltage excitation are plotted in Figure 3 for comparison. The solid line represents the identified model response and the dotted line depicts the system measured output response. It can be observed that the dynamic behavior of the identified model is matched with the suspension system dynamic response. The difference between both responses curves is due to the system nonlinear and time-varying behaviors. Based on this identified model, a model-based sliding-mode controller can be designed for the quarter-car active suspension system.

4. Controller Design

In this section, a model-based sliding-mode controller for the quarter-car suspension system is designed based on the model derived in section 3. The system control block diagram of the quarter-car active suspension system is shown in Figure 4. Firstly, the time-varying third order system model, equation (6), can be represented as the form

$$\begin{aligned} \ddot{x}_1(t) &= -A(t)\ddot{x}_1(t) - B(t)\dot{x}_1(t) - D(t)x_1(t) + G(t)u_s(t) \\ &= -(A_m + \Delta A)\ddot{x}_1(t) - (B_m + \Delta B)\dot{x}_1(t) \\ &\quad -(D_m + \Delta D)x_1(t) + (G_m + \Delta G)u_s(t) \end{aligned} \quad (7)$$

where A_m , B_m , D_m and G_m are the system model parameters and

$$\left\{ \begin{array}{l} |\Delta A| < \alpha \\ |\Delta B| < \beta \\ |\Delta D| < \gamma \\ 0 \leq \delta_{\min} = \frac{G_{\min}}{G_m} \leq \Delta G \leq \frac{G_{\max}}{G_m} = \delta_{\max} \end{array} \right. \quad (8)$$

where α , β and γ are the worse case values of the system model parameter variations.

The sliding surface for this third order system can be defined as

$$\begin{aligned} s &= \left(\frac{d}{dt} + \lambda\right)^2 x_1 \\ &= \ddot{x}_1 + 2\lambda\dot{x}_1 + \lambda^2 x_1 \end{aligned} \quad (9)$$

where the positive λ implies the convergent rate of x_1 on the sliding surface. Substituting equation (7) into the time derivative of s , obtain

$$\begin{aligned} \dot{s} &= \ddot{x}_1 + 2\lambda\dot{x}_1 + \lambda^2 x_1 \\ &= -(A_m + \Delta A)\ddot{x}_1 - (B_m + \Delta B)\dot{x}_1 - (D_m + \Delta D)x_1 \\ &\quad + (G_m \Delta G)u + 2\lambda\dot{x}_1 + \lambda^2 x_1 \end{aligned} \quad (10)$$

The control law u can be chosen as

$$\begin{aligned} u &= \frac{1}{G_m} [A_m \ddot{x}_1 + B_m \dot{x}_1 + D_m x_1 - 2\lambda\dot{x}_1 - \lambda^2 x_1 \\ &\quad - \eta_1 \operatorname{sgn}(s)] \end{aligned} \quad (11)$$

Substituting equation (11) into (10), obtain

$$\begin{aligned} \dot{s} &= (1 - \Delta G)[-A_m \ddot{x}_1 - B_m \dot{x}_1 - D_m x_1 + 2\lambda\dot{x}_1 + \lambda^2 x_1 \\ &\quad - \Delta A \ddot{x}_1 - \Delta B \dot{x}_1 - \Delta D x_1 - \Delta G \eta_1 \operatorname{sgn}(s)] \\ &= (1 - \Delta G)\hat{u} - \Delta A \ddot{x}_1 - \Delta B \dot{x}_1 - \Delta D x_1 - \Delta G \eta_1 \operatorname{sgn}(s) \end{aligned} \quad (12)$$

where

$$\hat{u} \equiv -A_m \ddot{x}_1 - B_m \dot{x}_1 - D_m x_1 + 2\lambda\dot{x}_1 + \lambda^2 x_1 \quad (13)$$

By multiplying the sliding variable s , the equation (12) can be written as

$$\begin{aligned} s\dot{s} &= (1 - \Delta G)\hat{u}s - \Delta A \ddot{x}_1 s - \Delta B \dot{x}_1 s - \Delta D x_1 s - \Delta G \eta_1 |s| \\ &\leq (1 - \delta_{\min})|\hat{u}|s + \alpha|\ddot{x}_1|s + \beta|\dot{x}_1|s + \gamma|x_1|s - \delta_{\min} \eta_1 |s| \end{aligned} \quad (14)$$

If the robustness parameter η_1 is selected as:

$$\begin{aligned} \eta_1 &\geq \frac{1}{\delta_{\min}} [(1 - \delta_{\min})|\hat{u}| + \alpha|\ddot{x}_1| + \beta|\dot{x}_1| + \gamma|x_1| + \eta_2] \\ \eta_2 &> 0 \end{aligned} \quad (15)$$

Then the equation (14) results in

$$s\dot{s} \leq -\eta_2 |s| < 0 \quad (16)$$

That means the system's stability can be achieved by choosing appropriate robustness gain constant η_1 . In addition, the control law $u(t)$, equation (11), can guarantee the system output error convergence.

5. Experimental Results

In order to investigate the control performance of the active suspension system with the proposed controller, a quarter-car hydraulic actuating active suspension system is constructed. Its mechatronics block diagram is shown in Figure 5. The whole system consists of an active suspension unit, a road profile simulator unit, a hydraulic power unit and a control unit. The first hydraulic servo system is employed to control the sprung-mass displacement and acceleration. The second hydraulic servo system is used to generate various road profiles for simulating the road surface variation. An optical linear scale and a linear potentiometer are installed to measure the vertical displacements of the sprung mass and road surface profile. The I/O interface includes a PCL-726 D/A card, a PCL-812 A/D card, and a PCL-833 card with onboard encoders to extract the output signal of the optical linear scale. A PC Pentium is used to handle all the I/O data

operation for the whole system and to suppress the vertical oscillation of the sprung mass with the designed turbo C control program.

This quarter-car experimental model is a serial type active vehicle suspension system. A sliding-mode controller is proposed to control this active suspension system. Since the feedback signals are liable to be disturbed by the environmental noise and it will be amplified during the numerical difference operation, a digital Butterworth filter and an RC filter circuit are introduced to solve this problem. The digital filter can be represented as

$$y_{out}(j) = 0.98y_{out}(j-1) + 0.01[y_m(j) + y_m(j-1)] \quad (17)$$

where $y_{out}(j)$ is the output signal of this digital filter and $y_m(j)$ is the sensor measuring data in response to the sprung mass position variation. The control signal is the input voltage of the eletro-servo valve. The control objective is to monitor the dynamic motion of the sprung mass.

In order to investigate the control performance of the proposed controller, the following experiments are performed. The sampling frequency is chosen as 100 Hz. Based on the system identification model, equation (6), the parameters $A_m = 60.14$, $B_m = 1487$, $D_m = 2824$ and $G_m = 12820$ are employed to design the model based sliding-mode controller. The converging parameter, η_2 , of the sliding surface reaching condition, equation (16), is chosen as 5000. Then, the appropriate robustness control parameter, η_1 , in the control law, equation (11), can be calculated from equation (15) based on 20% maximum variation of the system nominal parameters. Its estimation value for this hydraulic active suspension system is set as 6800. The parameter λ which influences the converging slope of the sliding surface was chosen as 15. The values of these control parameters are not critical for practical implementation.

Case A: The road surface profile is a step terrain.

When a vehicle is riding on a step terrain with

40 mm amplitude, the dynamic responses of the sprung mass position by using sliding-mode controller are shown in Figure 6. It can be observed that the maximum sprung mass displacement has been controlled to be less than 3.5mm. The root mean square (RMS) value of the sprung mass displacement is 0.78mm. Figure 7 shows the sprung mass acceleration by using the sliding-mode controller. It can be observed that the maximum sprung mass acceleration is 43 mm/s^2 and the RMS value of the sprung mass acceleration is 4.8 mm/s^2 .

Case B: The road surface profile is a concave-convex terrain.

When a vehicle is riding on a concave-convex terrain with 40 mm height as the dashed line shown in Figure 8, the dynamic response of the sprung mass position by using sliding-mode controller is plotted as solid line in Figure 8. It can be observed that the maximum sprung mass displacement has been controlled to be less than 5 mm. The root mean square (RMS) value of the sprung mass displacement is 1.7 mm. Figure 9 shows the sprung mass acceleration by using the sliding-mode controller. It can be observed that the maximum sprung mass acceleration is 65 mm/s^2 and the RMS value of the sprung mass acceleration is 11 mm/s^2 .

Case C: The road surface profile is a random terrain.

When a vehicle is riding on a random terrain as the dashed line shown in Figure 10, the dynamic response of the sprung mass position by using sliding-mode controller is plotted as solid line in Figure 10. It can be observed that the maximum sprung mass displacement has been controlled to be less than 4 mm. The root mean square (RMS) value of the sprung mass displacement is 1.15mm. Figure 11 shows the sprung mass acceleration by using the sliding-mode controller. It can be observed that the maximum sprung mass acceleration is 55 mm/s^2 and the RMS value of the sprung mass acceleration is 14.9 mm/s^2 . Hence, the passenger's riding

comfort is improved by using the proposed sliding-mode control strategy.

6. Conclusions

A sliding-mode controller is developed and successfully employed to control a quarter-car hydraulic active suspension system. The experimental results show that the designed controller has significantly suppressed the oscillation amplitude of the sprung mass for improving the riding comfort and handling capability. Hence, this control strategy is practical for vehicle active suspension system implementation.

References

- [1] A. Alleyne and J. K. Hedrick, "Nonlinear adaptive control of active suspensions," *IEEE Transactions on Control Systems Technology*, vol. 3, no. 1, pp. 94-101, 1995.
- [2] R. Rajamani and J. K. Hedrick, "Adaptive observers for active automotive suspensions: Theory and Experiment," *IEEE Transactions on Control Systems Technology*, vol. 3, no. 1, pp. 86-93, 1995.
- [3] E.-S. Kim, "Nonlinear indirect adaptive control of a quarter car active suspension," in *Proceedings of the 1996 IEEE International Conference on Control Applications*, Dearborn, MI, 1996, pp. 61-66.
- [4] S. Chantranuwathana and H. Peng, "Adaptive robust control for active suspensions," in *Proceedings American Control Conference*, 1999, pp. 1702-1706.
- [5] T. T. Nguyen, T. H. Bui, T. P. Tran and S. B. Kim, "A hybrid control of active suspension system using H_∞ and nonlinear adaptive controls," in *Proceedings IEEE International Symposium on Industrial Electronics*, 2001, vol. 2, pp. 839-844.
- [6] M. C. Smith and F.-C. Wang, "Controller parameterization for disturbance response decoupling: application to vehicle active suspension control," *IEEE Transactions on Control Systems Technology*, vol. 10, no.3, pp. 393-407, 2002.
- [7] I. Fialho and G. J. Balas, "Road adaptive active suspension design using linear parameter-varying gain-scheduling," *IEEE Transactions on Control Systems Technology*, vol. 10, no.1, pp. 43-54, 2002.
- [8] Sam YM, Osman JHS, Ghani MRA. A class of proportional-integral sliding-mode control with application to active suspension system. *Systems & Control Letters* 2004;51:217-223.
- [9] Kim C, Ro PI, Kim H. Effect of the suspension structure on equivalent suspension parameters. *Proceedings of the Institution of Mechanical Engineers*, part D 1999;213:457-470.
- [10] Kim C, Ro PI. A sliding-mode controller for vehicle active suspension systems with non-linearities. *Proceedings of the Institution of Mechanical Engineers*, part D 1998;212:79-92.
- [11] S. J. Huang and W. C. Lin, "Adaptive fuzzy controller with sliding surface for vehicle suspension control," *IEEE Trans. on Fuzzy Systems*, vol. 11, no. 4, pp. 550-559, 2003.
- [12] L. Ljung, *System identification toolbox for use with MATLAB*. The Mathworks Inc., 2000.



Figure 1 Hydraulic actuating quarter-car active suspension system

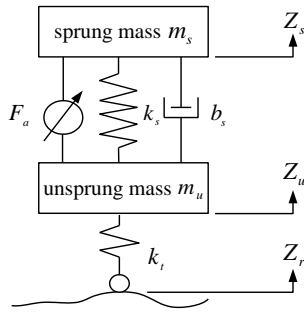


Figure 2 Active suspension system model

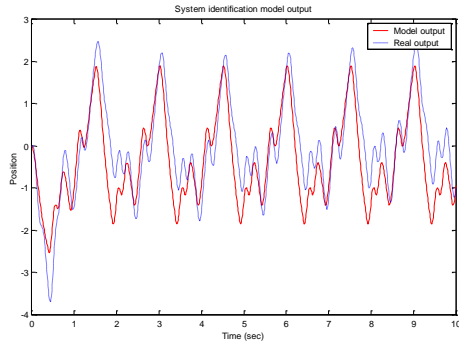


Figure 3 System identification model output

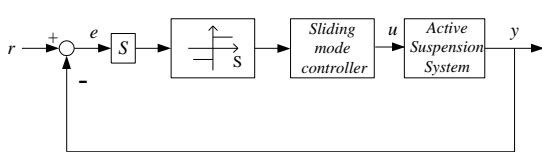


Figure 4 System control block diagram

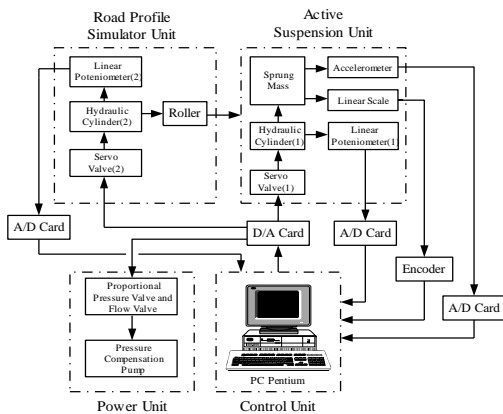


Figure 5 Mechatronics block diagram

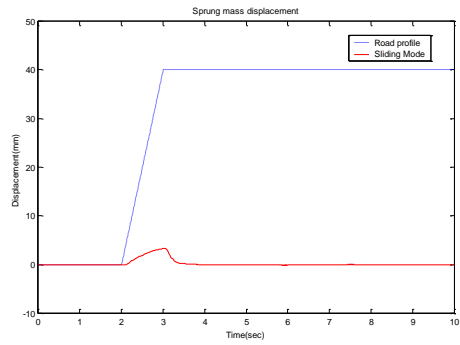


Figure 6 Sprung mass displacement (case A)

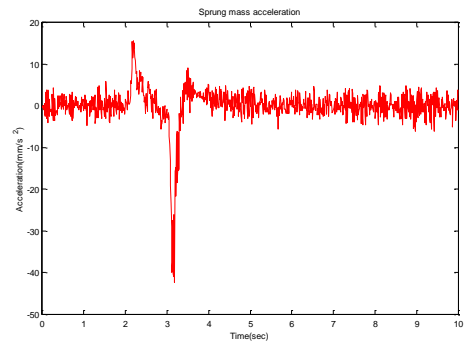


Figure 7 Sprung mass acceleration (case A)

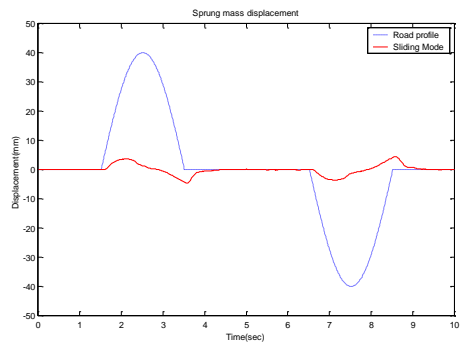


Figure 8 Sprung mass displacement (case B)

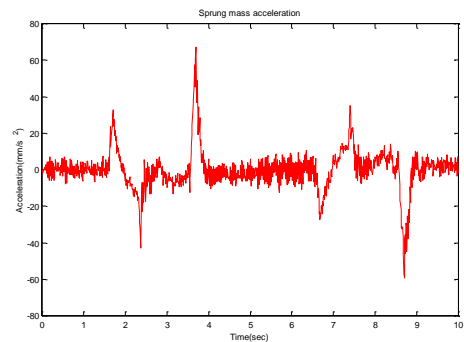


Figure 9 Sprung mass acceleration (case B)

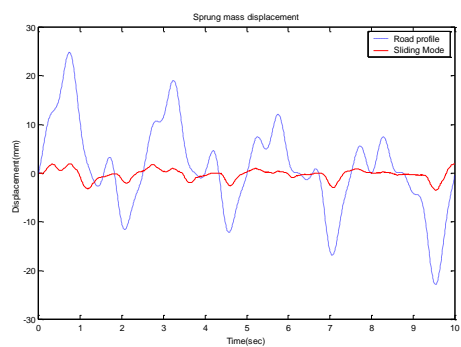


Figure 10 Sprung mass displacement (case C)

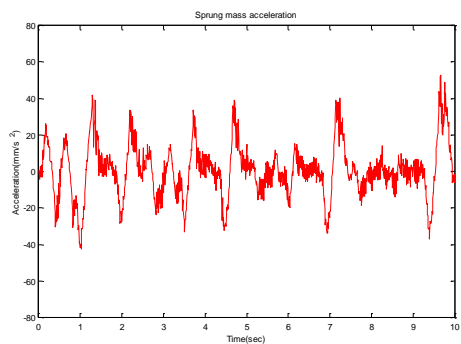


Figure 11 Sprung mass acceleration (case C)